Modeling Biochemical Reactions and Gene Networks with Memristors

Hanna Abo Hanna*, Loai Danial†, Shahar Kvatinsky†, and Ramez Daniel*
* Department of Biomedical Engineering
† Viterbi Faculty of Electrical Engineering
Technion - Israel Institute of Technology
Haifa 32000 ISRAEL
Email: shahar@ee.technion.ac.il, ramizda@bm.technion.ac.il

***Abstract*— This paper investigates qualitative and quantitative analogies between biochemical reactions and memristive devices. It shows that memristors can mimic biochemical reactions and gene networks efficiently, and capture both deterministic and stochastic dynamics at the nanoscale level. We present different abstraction models and memristor-based circuits that inherently model the activity of genetic circuits with low signal-to-noise ratio (SNR). These findings constitute a promising step towards noise-tolerant and energy-efficient electronic circuit design, which can provide a fast and simple emulative framework for large-scale synthetic molecular system design in cell biology.**

***Keywords*—Cytomorphic, genetics, memristors, molecular biology, synthetic biology, systems biology.**

I. Introduction

Cytomorphic electronics is a novel field of designing noise-tolerant ultra-low power cell-inspired circuits [1]. The main goals of this field are to simulate cells, organs, and tissues while considering the stochastic behavior of a single cell and cell-to-cell variation, distortion, and cross-talk using mixed-signal integrated electronics. Such simulations are computationally intensive and can take weeks using modern digital hardware. Additionally, cytomorphic electronics is used to design novel large-scale synthetic biological systems [2] by providing a fast and simple emulative framework. Furthermore, the field has aided in the design of electronic circuits and networks inspired by molecular biology, with uniquely emergent characteristics and concepts to be adopted for energy-efficient hardware realization.

Recently, it has been shown that translinear electronics-based subthreshold MOS transistors can efficiently represent molecular circuits within the cell [3][4]. However, it was challenging to capture the random fluctuations of molecular and genetic circuits that involve a small number of proteins, such as those in DNA-protein binding reactions, using an analog transistor. Therefore, standalone artificial noise generation circuits for signal-to-noise ratio (SNR) below 10 dB [4] were required. Such circuits produce artificial random fluctuations that are represented as a Poisson process, and scale as the square-root of the current count. Artificial noise generation circuits were created by pseudo-random digital noise generation [1] or by amplifying the intrinsic thermal noise in analog transistors [4]. Such systems often involve many analog and digital circuits, such as a current-controlled oscillator and a linear shift frequency register, which makes scalable cytomorphic integrated electronics more difficult to design. In this paper, we propose a different approach that exploits the stochastic nature and deterministic dynamics of two terminal nanoscale emergent devices, known as memristors [6], integrated into an analog MOS transistor to model the dynamic fluctuations of biochemical reactions and genetic circuits within the cell.

The analogy of memristive devices and biochemical binding reactions is made at the biophysical dynamic and energy level. Early efforts to construct gene networks in living cells have used binding and unbinding reactions to represent two logic states, "ON/OFF" or "1/0" [8]. Consequently, the dynamics of a binding reaction depend upon the flow of proteins toward the active binding site where the new complex is formed. By analogy and as illustrated in Fig. 1(a), the migration of oxygen vacancies in solid-state memristors (metal-insulator-metal structure) towards the undoped region forms a conductive filament. When programming voltage pulses are applied on the memristor, its resistance switches between two logic states: high resistance state (HRS) and low resistance state (LRS). This similarity is illustrated in Fig. 1(b), where the free energy of the binding reaction [1] and ionic species in solid-state memristors are described by a thermal activated process [10]. Protein concentration P controls the energy barrier of a biochemical binding reaction, exponentially changing its speed. Correspondingly, the programming voltage controls the energy barrier of ionic species between OFF and ON states. Then protein concentration maps naturally to the number of programming pulses.

Recently there has been widespread interest in memristive technologies because of their potential to enable a wide range of applications, *e.g.*, non-volatile memory, programmable logic, analog computations, and neuromorphic computing where memristors mimic synapses [7]. In this paper, we show a new feature of memristive devices—their ability to mimic biochemical binding reactions, demonstrating a novel application in the field of cytomorphic electronics.

II. Modeling

A. The Linear Model - Motivation

In the inset of Fig.2 we see a simple biochemical reaction of protein P that binds to a binding site to form a new complex P*.

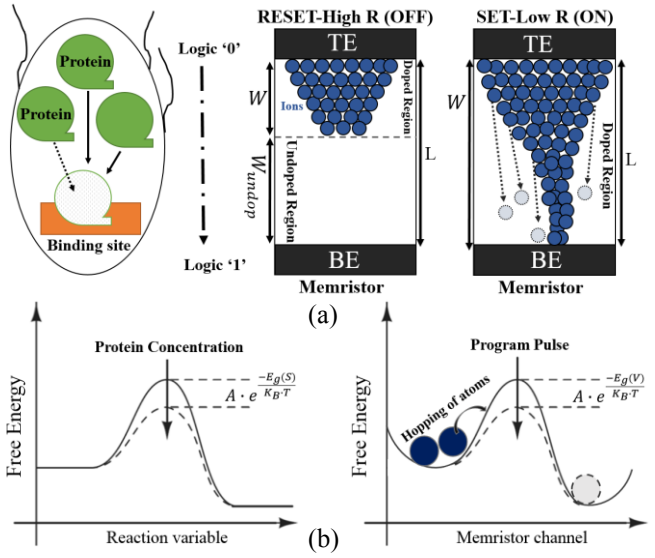

Fig. 1. (a) Analogies between biochemical binding reactions and memristive devices. The SET process results in LRS ('1'), and the RESET in HRS ('0'). (b) Analogies between molecular flux in chemical reactions and ionic species flow in memristive devices.

As a first order approximation, the concentration of the formed complex can be given as a linear reaction

$$dP^*/dt = \alpha \cdot N_T \cdot P, \tag{1}$$

$$N + P^* = N_T\,. \tag{2}$$

The first expression describes the chemical kinetics rate of production of a new complex P^* with rate α, and (2) can be viewed as a molecular balance law, where N_T is the concentration of the total number of binding sites, N is the concentration of the total number of free binding sites, and P is the protein concentration. A simple solution for (1) and (2) shows that the concentration of the new complex has two levels (zero, and N_T), which can be denoted by ON and OFF, respectively. In other words, the biochemical reaction consists of a free and occupied binding sites, which can be viewed as time-dependent internal state variables whose sum is constant. The protein concentration changes this fraction. Figure 1(a) shows the physical structure of the memristive device. The semiconductor thin film has a certain length L, and consists of a doped (w) and undoped region (w_{un_dop}) [6]. The internal state variable w represents the length of the doped region. The doped region has a low resistance while that of the undoped region is much higher. As an external current bias, $I(t)$, is applied across the device, the length of w will change. As a first order approximation, the length of the memristor can be described by a linear model as

$$dw/dt = (\mu/L) \cdot R_{ON} \cdot I(t)\,, \tag{3}$$

$$L = w + w_{undop}\,, \tag{4}$$

where μ is the mobility of ionic species in the solid-state device. If the doped region extends to the full-length L, the total resistivity of the device will be dominated by a low resistivity region, with a value measured to be R_{ON}. Likewise, when the undoped region extends to the full-length L, the total resistance is denoted as R_{OFF}. The set of equations (1) and (2) is equivalent

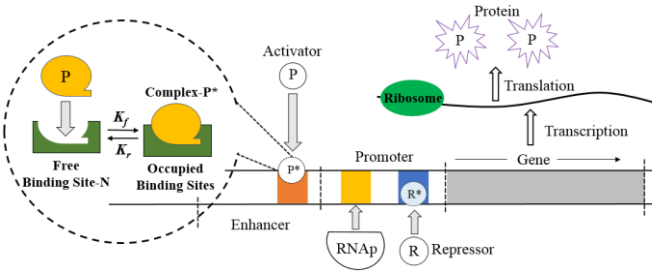

Fig. 2. A simplified overview of the process of binding reaction, transcription and translation in a bacterial genetic circuit. Inset Figure 2 shows the biochemical reaction between protein P (Activator/Repressor) and its binding site to form a new complex P^* *or* R^*.

to the set of equations (3) and (4), because both involve the motion of charged atomic or molecular species, including state variable dependency on time. Therefore, the similarity between memristors and biochemical reactions has been observed at the physical nano-scale level.

B. The Non-Linear Model

Biochemical reactions often include two reactions that occur simultaneously [8]: a forward reaction with rate k_f that enhances the reaction, and a reverse reaction with rate k_r that inhibits the reaction, as illustrated in the inset of Fig. 2. This process is described by modifying (1) to

$$dP^*/dt = k_f \cdot N_T \cdot P - \left(k_r + k_f \cdot P\right) \cdot P^*\,. \tag{5}$$

Assuming that $P \gg N_T$, a simple solution for (5) and (2) in steady state is

$$P^* = N_T \cdot \frac{P}{P+\gamma}\,, \tag{6}$$

where $\gamma = k_r/k_f$. γ has units of concentration and is known as the dissociation constant of the biochemical reaction. This solution is known as Michaelis-Menten kinetics, and it can be modeled by Kirchhoff's current law (KCL) and a resistive current divider between resistors with values P and γ respectively, where N_T is the current source and P^* is the current that is passed through the R_γ resistor. The circuits shown in Fig. 3 model the non-linear behavior of biochemical reactions. We replace the resistor P with a memristor that is controlled by programming voltage pulses with a constant width. In this configuration, the memristor operates in the analog mode with multiple resistance levels and the programming pulses set the memristance. For simplicity, we use the linear ion drift mode [9] to express the memristance, which is given by

$$R_M = (R_{OFF} - R_{ON}) \cdot \frac{w - W_{ON}}{L - W_{ON}} + R_{ON}, \tag{7}$$

$$dw/dt = K_{off} \cdot \frac{(V(t) - V_{off})}{V_{off}}, \tag{8}$$

where W_{ON} is the width of the doped region in the ON state, K_{off} is a velocity constant with units of *nm/sec*, and V_{off} is an internal voltage that is proportional to R_{ON}. For N_P programming pulses with pulse period T_P, and amplitude A_V, the memristance is approximately

$$R_M = R_{ON} + R_0 \cdot N_p, \tag{9}$$

$(W/L)_{1,2}$	40µm/0.18µm
k_{off}/k_{on}	$\pm 1mm/s$
α_{off}/α_{on}	1
R_{on}	100 Ω
R_{off}	800 $k\Omega$
V_{off}	10 V
L	10 nm
V_A	11 V
T_P	212 nsec
I_T	100μA

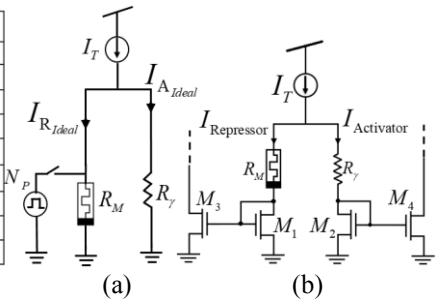

Fig. 3. Memristor based electronic circuits using VTEAM memristor model and 0.18um CMOS to model the behavior of the non-linear model of biochemical reactions. (a) Standalone ideal circuit and (b) within a network circuit.

where $R_0 = (R_{OFF} - R_{ON}) \cdot K_{off} T_P \cdot (A_V - V_{off})/(L \cdot V_{off})$. By substituting (9) into the KCL, the current passed through the γ resistor is expressed as

$$I_{Activator} = I_T \frac{N_P}{N_P + R_{ON}/R_0 + R_\gamma/R_0} + I_T \frac{R_{ON}/R_0}{N_P + R_{ON}/R_0 + R_\gamma/R_0} \quad (10)$$

Equation (10) has two terms. The left term fits the model of the biochemical binding reaction (6), where the dissociation constant $\gamma = R_{ON}/R_0 + R_\gamma/R_0$ denotes that the increase in the number of programming pulses will increase the current until saturation with value of I_T, where $N_P \gg R_{ON}/R_0 + R_\gamma/R_0$. The right term is a leakage current; when $N_p = 0$, then $I_{Activator} \neq 0$. This is known as the basal level that is often present in biochemical binding reactions [8].

C. Memristor Models of Promoter Activity in Genetic Circuits

Fig. 2 shows two types of proteins that bind to DNA binding sites within the promoter [8] in genetic circuits: activators, which enhance the binding of RNA polymerase (RNAP) responsible for the transcription process (production of RNA), and repressors, which inhibit the promoter activity by preventing the RNAP from binding to the promoter. In activation, transcription is often followed by a translation process and the production of proteins. Activation is often modeled by (6) (simulation results are shown in Fig. 4(a)), while repression is modeled by the concentration of the free binding sites N and is expressed as

$$N = N_T - P^* = N_T \cdot \frac{\gamma}{P+\gamma}. \quad (11)$$

Expression (11) can be viewed as the difference between the total current and the current that is passed through the γ resistor, which is equal to the current that is passed through the memristor:

$$I_{Repression} = I_T \frac{R_\gamma/R_0}{N_p + R_{ON}/R_0 + R_\gamma/R_0}, \quad (12)$$

where $\gamma = R_\gamma/R_0$ is the dissociation constant, and R_{ON}/R_0 is the basal level in repression ($N_P = 0$). Simulation results are shown in Fig. 4(b)

D. The Stochastic Model

Signals often originate from the transport of discrete random carriers. In subthreshold transistors, such signals arise from the diffusion of electrons, and in biology from the diffusion of biochemical molecules and proteins. These signals prorogate with random fluctuations. These fluctuations are known as

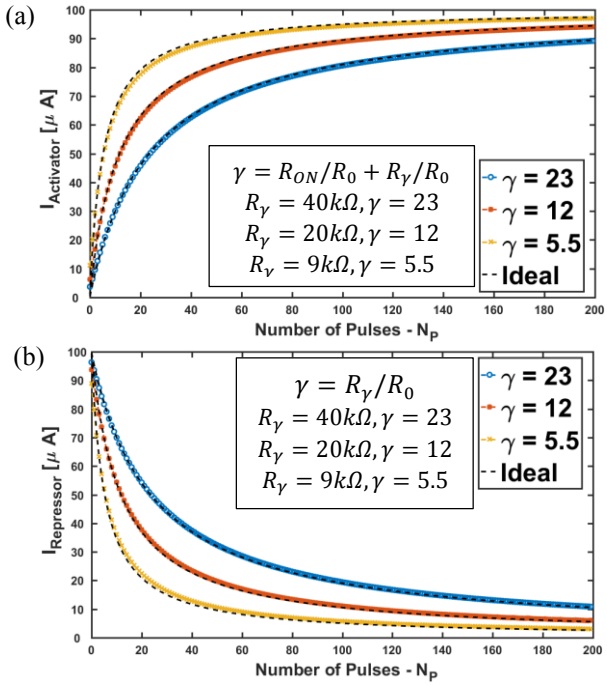

Fig. 4. SPICE simulations for different values of $\boldsymbol{\gamma}$ for the circuits from Fig. 3(b). The value of $\boldsymbol{\gamma}$ is controlled by changing $\boldsymbol{R_\gamma}$. (a) Activator concentration versus number of pulses. (b) Repressor concentration versus number of pulses. The ideal (dashed line) curves represent the current $\boldsymbol{I_{A_{Ideal}}}$ and $\boldsymbol{I_{R_{Ideal}}}$ in the standalone circuit from Fig. 3(a) for each activator and repressor accordingly, and the solid curves represent the current $I_{Activator}$ and $I_{Repressor}$ in Fig. 3(b).

intrinsic noise through networks and can be described as a Poisson process, generating shot noise which scales as the square-root of the molecular count [5]. The rate coefficients of chemical reactions are often described by Boltzmann statistic $K = A \cdot \exp(-E_g/K_B \cdot T)$, are exponential in free energy difference in chemical reactions, and an increase in enzyme concentration decreases energy barriers, as shown in Fig. 1 (b). Recently it has been shown that the rate of switching in memristor devices is determined by bias-dependent activation energy [10], follows Boltzmann statistics $\Gamma = A \cdot \exp(-E_V/K_B \cdot T)$, and an increase in voltage decreases energy barriers, as also shown in Fig. 1(b). This simple analysis shows that the effective binding time of proteins and the delay time of switching memristors both follow a Poisson distribution. Therefore, the stochastic noise in biochemical reactions is analogous to the stochastic noise in memristor switching. These analogies suggest that one can mimic and model large-scale genetic-processing systems in biological networks efficiently on a hybrid memristor-analog-digital electronic chip. Equation (9) shows that the memristor acts as an analog counter of the arrival pulses during programming. The stochastic kinetics of a pulse counter often follow Poisson shot noise statistics when the variance is equal to the mean (*e.g.*, photon counting). Simplified analog transistor models are useful in the design and analysis of practical electronic systems since they quantitatively represent their behavior. Fig. 5 shows a circuit that receives programming pulses and measures the output voltage of a common drain (CD) amplifier (buffer). In steady state, the voltage is

$$V_{out_{CD}} = I_M \cdot (R_0 \cdot N_P + R_{ON} + R_a). \quad (13)$$

k_{off}/k_{on}	$\pm 1\mu m/s$
α_{off}/α_{on}	1
R_{on}	$1\ k\Omega$
R_{off}	$11\ k\Omega$
V_{off}	$4\ V$
V_A	$4.5\ V$
T_P	$40\mu sec$
I_m	$20\mu A$
I_0	$1.5 - 1.7\ x10^{-4} A$
R_a	$104\ k\Omega$

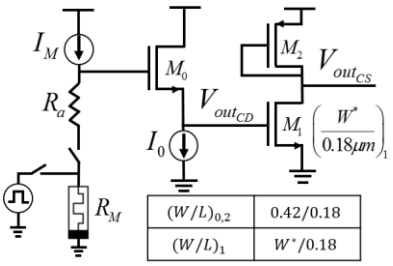

$(W/L)_{0,2}$	0.42/0.18
$(W/L)_1$	$W^*/0.18$

Fig.5. Memristor based electronic circuit to capture the deterministic and stochastic behavior of biochemical reactions. The first stage, the common drain, represents the transcription process, whereas the second stage, the common source, amplifies the noise and captures the burst size; this stage represents the translation process. The gain value is controlled by the transistor width $\boldsymbol{W^*}$.

We define the output v_{mRNA} as the difference between the voltage for any number of programming pulses N_P, and the voltage for N_P=*0*:

$$v_{mRNA} = V_{out_{CD}} - V_{out_{CD_0}} = I_M \cdot R_0 \cdot N_P \,. \quad (14)$$

If N_P is controlled by a "random clock", the SNR of the output is proportional to the SNR of the random clock. Then, the process of counting of these pulses or events by the proposed circuit in Fig. 5 exhibits pure Poisson characteristics with variance of N_P that is equal to the mean. Then the SNR in the output is

$$SNR_{v_{mRNA}} = \overline{v_{mRNA}} / \sqrt{\overline{\Delta v_{mRNA}{}^2}} = \sqrt{\overline{N_P}} \,. \quad (15)$$

In our configuration, the number of programming pulses is analogous to the promoter activity, which is set by the binding of RNAP to DNA [8], and the output v_{mRNA} is analogous to mRNA concentration. Approximately, the expression of mRNA can be viewed as the counting process of arrival RNAP to the promoter with variance that is equal to the mean ($\overline{\Delta mRNA^2} = \overline{mRNA}$) [5]. Correspondingly, the common drain output voltage is the counting process of programming pulses on the memristor. Translation is the process of converting RNA to amino acids and protein production [8]. This process can be viewed as a first order approximation, as a process of counting the arrival of ribosomes to mRNA; therefore, this is a stochastic process that follows Poisson statistics. However, biological experiments and biophysical models show that the variance of protein is larger than the Poisson statistic ($\overline{\Delta Protein^2} = (1 + b) \cdot \overline{Protein}$) [5]. The parameter b in biology is known as the burst size and is equivalent to the number of proteins synthesized from a single mRNA transcript [5]. If b is large, a single mRNA molecule is recycled several times before it degrades. Therefore, the burst size is the molecular gain from mRNA to protein, which amplifies the mRNA noise content in the protein signal. Figure 5 shows a circuit that can amplify the noise through a common source (CS) amplifier and capture the burst size. Simulation results are shown in Fig. 6. Similarly, we define the output of the CS amplifier as the difference between the voltage for any number of programming pulses N_P and the voltage for N_P=*0*. The output $v_{protein}$ represents the protein concentration with statics

$$v_{protein} = -(gm_1/gm_2) \cdot I_M \cdot R_0 \cdot N_P. \quad (16)$$

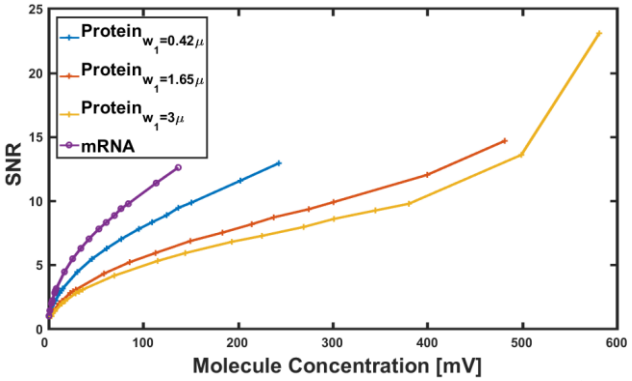

Fig. 6. SPICE simulations of SNR versus molecule concentration ($\overline{v_{mRNA}}$, $\overline{v_{Protein}}$) accordingly, for different gains (1.7, 3.5 and 4.5) of the circuit from Fig. 5. The CS stage amplifies the noise and results in lower SNR in contrast to the CD stage. $\boldsymbol{gm_1/gm_2}$ represents the $(\boldsymbol{1 + b})$ factor**.** Second-order effects start to have significant impact as the gain becomes higher.

Simulation results are shown in Figure 6.

III. Conclusions

We demonstrate the analogies between memristor devices and biochemical reactions at the nanoscale physical level and propose different models that capture the deterministic and stochastic dynamics of biochemical reactions and gene networks by memristor-based electronic circuits, while achieving low signal-to-noise ratio. These circuits are the first step towards the design of novel, cell-inspired, energy-efficient electronic circuits that provide a fast and simple conceptual framework for emulation of large-scale stochastic synthetic biological systems. In our ongoing research, we are comparing the memristor based electronic circuits with biological experimental data.

References

[1] R. Sarpeshkar, "Cytomorphic Electronics: Cell-inspired Electronics for Systems and Synthetic Biology." *Ultra Low Power Bioelectronics: Fundamentals, Biomedical Applications, and Bio-inspired Systems*, Cambridge University Press, Cambridge, U.K. 2010, ch 24, pp. 753– 786.

[2] R. Daniel, J. R. Rubens, R. Sarpeshkar, and T. K. Lu, "Synthetic Analog Computation in Living Cells," *Nature*, Vol. 497, pp. 619–623, May 2013.

[3] R. Danial, S. S. Woo, L. Turicchia, and R. Sarpeshkar, "Analog Transistor Models of Bacterial Genetic Circuits," in *Proceedings of the IEEE Symposium on Biological Circuits and Systems,* pp. 333–336, November 2011.

[4] S. S. Woo, J. Kim, and R. Sarpeshkar, "A Cytomorphic Chip for Quantitative Modeling of Fundamental Biomolecular Circuits," *IEEE Transactions on Biomedical Circuits and Systems*, Vol.9, No. 4, pp. 527-542, August 2015.

[5] A. Eldar and M. B. Elowitz, "Functional Roles for Noise in Genetic Circuits," *Nature*, Vol. 467, No. 7312, pp. 167–173, September 2010.

[6] D. B. Strukov, G. S. Snider, D. R. Stewart, and R. S. Williams, "The Missing Memristor Found," *Nature*, Vol. 453, pp. 80–83, May 2008.

[7] S. H. Jo *et al*., "Nanoscale Memristor Device as Synapse in Neuromorphic Systems," *Nano Letters*, Vol. 10, No. 4, pp. 1297– 1301, April 2010.

[8] U. Alon, "An Introduction to Systems Biology: Design Principles of Biological Circuits," *Chapman Hall/CRC Mathematical and Computational Biology Series*, Vol. 10, No. 10. p. 301, 2007.

[9] S. Kvatinsky, M. Ramadan, E. G. Friedman, and A. Kolodny, "VTEAM: A General Model for Voltage-Controlled Memristors," *IEEE Transactions on Circuits and Systems II: Express Briefs*, Vol. 62, No. 8, pp. 786–790, August 2015.

[10] S. H. Jo, K. H. Kim, and W. Lu, "Programmable Resistance Switching in Nanoscale Two-Terminal Devices," *Nano Letters*, Vol. 9, pp. 496–500, January 2009.